

Article

Active Packaging Films Made by Complex Coacervation of Tragacanth Gum and Gelatin Loaded with Curcumin; Characterization and Antioxidant Activity

Fateme Amani ¹, Atefe Rezaei ^{1,*}, Hajar Akbari ¹, Cristian Dima ² and Seid Mahdi Jafari ^{3,4,5,*}

- ¹ Nutrition and Food Security Research Center, Department of Food Science and Technology, School of Nutrition and Food Science, Isfahan University of Medical Sciences, Isfahan P.O. Box 81746-73461, Iran
- ² Faculty of Food Science and Engineering, “Dunarea de Jos” University of Galati, “Domneasca” Str. 111, Building F, Room 107, 800201 Galati, Romania
- ³ Department of Food Materials and Process Design Engineering, Gorgan University of Agricultural Sciences and Natural Resources, Gorgan P.O. Box 49138-15739, Iran
- ⁴ Nutrition and Bromatology Group, Department of Analytical Chemistry and Food Science, Faculty of Science, Universidade de Vigo, E-32004 Ourense, Spain
- ⁵ College of Food Science and Technology, Hebei Agricultural University, Baoding 071001, China
- * Correspondence: atefe.rezaei@nutr.mui.ac.ir (A.R.); smjafari@gau.ac.ir (S.M.J.)

Abstract: The development of biopolymer-based green packaging films has gained remarkable attention in recent years. In this study, curcumin active films were prepared using different proportions of gelatin (GE) and a soluble fraction of tragacanth gum (SFTG) (1GE:1SFTG and 2GE:1SFTG) by complex coacervation. The various ratios of used biopolymers did not significantly impact the mechanical properties, thickness, and WVP of final films. However, biopolymers' ratio impacted the moisture content, water solubility, swelling ratio, and release rate. Blending curcumin with biopolymers caused a reduction in tensile strength (from 1.74 MPa to 0.62 MPa for film containing 1GE:1SFTG and from 1.77 MPa to 0.17 MPa for film containing 2GE:1SFTG) and proliferation in elongation at break (from 81.48% to 122.00% for film containing 1GE:1SFTG and from 98.87% to 109.58% MPa for film containing 2GE:1SFTG). Moisture content and water solubility of films experienced a decrease after the addition of curcumin. Antioxidant activity of curcumin-loaded films was almost five times higher than neat film samples. Furthermore, the interreaction between the carboxylic group of SFTG and amide I of GE formed an amide linkage and was proven by FTIR analysis. TGA showed a drop in the thermal stability of film samples compared to the main ingredients. In general, the complex coacervate of SFTG and GE has the advantage of developing eco-friendly and low-cost packaging film in the food industry, especially for the protection of fatty foods.

Keywords: tragacanth gum; gelatin; curcumin; complex coacervates; biodegradable packaging



Citation: Amani, F.; Rezaei, A.; Akbari, H.; Dima, C.; Jafari, S.M. Active Packaging Films Made by Complex Coacervation of Tragacanth Gum and Gelatin Loaded with Curcumin; Characterization and Antioxidant Activity. *Foods* **2022**, *11*, 3168. <https://doi.org/10.3390/foods11203168>

Academic Editor: Frédéric Debeaufort

Received: 15 September 2022

Accepted: 10 October 2022

Published: 11 October 2022

Publisher's Note: MDPI stays neutral with regard to jurisdictional claims in published maps and institutional affiliations.



Copyright: © 2022 by the authors. Licensee MDPI, Basel, Switzerland. This article is an open access article distributed under the terms and conditions of the Creative Commons Attribution (CC BY) license (<https://creativecommons.org/licenses/by/4.0/>).

1. Introduction

The adverse effects of using synthetic polymers and plastics in food packaging has raised concerns about environmental contamination and endangering wildlife. In addition, toxic chemical constituents of plastic packaging may leach into food and cause devastating effects on human health. Biopolymer-based packaging has been considered as a potential eco-friendly and nontoxic alternative to plastic films [1–3]. Different bio-based materials (protein, polysaccharide, and lipids) have the potential to be developed into biodegradable packaging materials [4].

Gelatin (GE) is known as a safe, low-price, and biodegradable polymer with film-forming properties. Additionally, GE can easily absorb UV light because of aromatic amino acids in its structure [5]. Due to some drawbacks, such as low thermal stability and poor mechanical and barrier properties, this biopolymer should be combined with other natural ingredients to present more desirable qualities [6]. Tragacanth gum (TG)

is an acid-resistant anionic biopolymer obtained from dried sap of *Astragalus* species. It contains water-swellaible and water-soluble parts. The hydrophilic nature of TG causes stabilizing and emulsifying properties and makes it a suitable constituent in the food and drug industries [7–9].

Proteins and polysaccharides can interact noncovalently and form coacervates or soluble complexes. The main driving forces for the noncovalent bonds are electrostatic, van der Waals, hydrogen bonding, and hydrophobic interactions [10]. Since most natural polysaccharides have negative charge and proteins have a positive charge at the pH values lower than their isoelectric point, stronger complexations of proteins and polysaccharides are expected [11]. Coacervation is the separation into two liquid phases in colloidal systems. The more concentrated phase is the coacervate, and the equilibrium solution is the other phase [12]. According to previous studies, complex coacervation is a potential technique in food packaging [13–15].

Due to the increasing concern of consumers over various side effects of synthetic preservatives, current studies have focused on producing active packaging films loaded with natural bioactive compounds including essential oils, plant extracts, and curcumin. Curcumin is the main polyphenolic compound in turmeric rhizomes (*Curcuma longa* Linn). The potential antimicrobial and antioxidant capacity of curcumin make it a favorable option for application in active food packaging [16,17]. Additionally, some studies on animals and humans have proven its safety and nontoxicity [18].

The current work aimed to prepare a biodegradable active film from GE and SFTG containing curcumin using complex coacervation. The effects of curcumin on mechanical, antimicrobial, antioxidant, and barrier properties of GE/SFTG films were investigated. Moreover, curcumin release rate from the blended films into fatty food simulants (50% ethanol, *v/v*, that was recommended by the US Food and Drug Administration) was evaluated.

2. Materials and Methods

2.1. Materials

Curcumin was bought from Merck (Darmstadt, Germany). TG was purchased from a local market in Isfahan, Iran. Type B GE (225 g bloom) was received from Amstel company, Netherlands. 2,2-Diphenyl-1-picrylhydrazyl (DPPH) was provided from Sigma Aldrich (Saint Louis, USA). Muller-Hinton Agar (MHA) and Muller-Hinton Broth (MHB) were purchased from QUELAB, Canada. The cultures of *Staphylococcus aureus* (ATCC:25923), *Bacillus cereus* (ATCC 11778), *Salmonella* Typhi (ATCC 19430), and *Escherichia coli* (ATCC 35150) were provided by the Pasteur Institute (Tehran, Iran). All other chemicals were of analytical grade.

2.2. Preparation of Soluble Fraction of TG

A specific amount of TG (0.25% *w/v*) was dissolved in distilled water and kept in the refrigerator overnight to complete hydration. For separating soluble and insoluble fractions of TG, the solution was centrifuged (MPW Med, MPW-206R, Warsaw, Poland) at 5500 rpm for 1 h. Then, the supernatant was dried at 50 °C to obtain the soluble fraction of TG (SFTG) [19].

2.3. Preparation of Complex Coacervates

Complex coacervates of GE and SFTG were prepared according to Devi and Maji [20]. The solutions of GE and SFTG were prepared in distilled water at 50 °C, separately. In the next step, different ratios of GE (1% *w/w*) and SFTG (1% *w/w*) solutions were mixed at 50 °C (Table 1). Solutions were stirred for 30 min, followed by adjusting the pH to 3.6 using acetic acid (10% *v/v*). Mixtures were stirred for 1 h and kept in the refrigerator overnight. To separate the sedimented part (complex coacervates) of the mixtures, samples were centrifuged at 5500 rpm for 30 min. Eventually, the obtained complex coacervates were dried using a freeze dryer (Dena Vacuum, Tehran, Iran) at −40 °C for 24 h.

Table 1. Different formulations of complex coacervates between gelatin (GE) and soluble fraction of tragacanth gum (SFTG).

Biopolymer Ratios (<i>w/w</i>)	Particle Yield (%)
1GE: 1SFTG	46.57 ± 1.71 ^b
2GE: 1SFTG	60.06 ± 0.14 ^a
1GE: 2SFTG	14.33 ± 0.81 ^c

Different letters indicate significant differences ($p < 0.05$).

To obtain the optimum biopolymers' ratio for the production of films, the particle yield (PY) was evaluated by the gravimetric method. To this end, the primary weight of biopolymers (M_0) and the obtained weight of dried complex coacervates (M_1) were measured; PY was calculated by Equation (1).

$$PY (\%) = (M_1 / M_0) \times 100 \quad (1)$$

The samples with higher PY were used for the production of films containing curcumin.

2.4. Film Formation Process

The preparation of films was by casting method according to Eghbal et al., (2016) [14]. Complex coacervates powder (6% *w/w*) was completely dissolved in acetate buffer (pH = 3.6) at room temperature. Curcumin (0.3% dry weight) was added to the mixture and stirred overnight. Then, glycerol (35% dry weight) was added to the mixture as a plasticizer and stirred for 1 h. CaCl_2 (1% *w/v*) as a cross-linking agent was also added and mixed for 5 h. The film without curcumin was prepared as a blank sample the same as above. Finally, 20 mL of the final solution was poured into a plate (90 mm diameter) and dried at room temperature (25 °C) and ambient relative humidity (RH = 45%) for 48 h.

2.5. Characterization of Films

2.5.1. The Thickness and Mechanical Properties

To report the mean value of thickness, five random positions of produced films were quantified using a digital micrometer (Mitutoyo, Kawasaki, Kanagawa, Japan) with the accuracy of 0.001 mm. A texture analyzer (SANTAM STM-1, Tehran, Iran) with a 50 N load cell based on the ASTM method [21] was applied to assess mechanical properties. For this purpose, strips of films in dimensions of 70 mm × 10 mm were provided. Measurements were performed with an initial gap of 30 mm and a cross-head speed of 5 mm/s. Tensile strength (TS) and elongation at break (EAB) of the samples were calculated according to Equations (2) and (3), respectively.

$$TS \text{ (MPa)} = \frac{F}{d \times w} \quad (2)$$

$$EAB (\%) = \frac{E - E_0}{E_0} \times 100\% \quad (3)$$

where F is the maximum tension (N) when the films are broken, d is the thickness (mm) of films, w is the width (mm) of films, E is the length (mm) of film at rupture, and E_0 is the initial length (mm) of films. The mechanical measurements were performed in triplicate, and the mean values were reported.

2.5.2. Water Vapor Permeability (WVP)

The ASTM E96 method [22], based on the gravimetric method, with slight modification, was considered to determine WVP. Each test tube, with 10 mm internal diameter and 55 mm depth, contained 1 g CaCl_2 (0% relative humidity, RH) and was sealed with the films. Then, all test tubes were placed in the desiccator with a RH = 75% and were incubated at 45 °C. To maintain 75% RH, a constant mass of a saturated solution of NaCl was used in a

desiccator (Boeckel, Hamburg, Germany). The test tubes were weighed every 24 h for 7 days. Equations (4) and (5) were used to calculate water vapor transmission rate (WVTR, g/day m²) and WVP (g mm/kPa day m²) of the films, respectively [23].

$$\text{WVTR} = \Delta m / (t \times A) \quad (4)$$

$$\text{WVP} = (\text{WVTR} \times l) / (\Delta P \times (\text{RH}_1 - \text{RH}_2)) \quad (5)$$

where l is the average thickness of the films (mm), A is the area of the test tube mouth (m²), ΔP is the vapor pressure difference (kPa), $\text{RH}_1 - \text{RH}_2$ is the RH difference across the films, and $\Delta m/t$ is the slope of the weight change versus time (g day⁻¹), which was calculated using linear regression ($r^2 \geq 0.99$).

2.5.3. Moisture Content (MC) and Water Solubility

The MC was estimated gravimetrically. Each film sample (2 × 2 cm²) was dried in the oven at 105 °C until a stable weight. Equation (6) was applied to determine MC. The dried film samples, which were utilized to assess MC, were immersed in beakers containing 20 mL distilled water for 24 h at room temperature. The undissolved films were taken out from the water and dried at 105 °C to reach a steady weight. Equation (7) was used to compute water solubility [24]:

$$\text{MC} (\%) = ((W_0 - W_1) / W_0) \times 100 \quad (6)$$

$$\text{Water solubility} (\%) = ((W_1 - W_2) / W_1) \times 100 \quad (7)$$

where W_0 is initial weight of film samples, W_1 is initial dry weight, and W_2 is final dry weight.

2.5.4. The Swelling Test

To measure the swelling rate of films in water, 2 × 2 cm² pieces of each sample film were separated, weighed, and soaked in distilled water. Then, the film pieces were removed from distilled water and dried with a cloth to remove excess water. The swelling degree (Equation (8)) of films was determined for 2 h with 10 min intervals by the gravimetric method [25]:

$$\text{Swelling ratio (g/g)} = (W_2 - W_1) / W_1 \quad (8)$$

2.5.5. Curcumin Release from Films

Curcumin release was evaluated in 50% ethanol as a simulant for fatty or oily foods [26]. At first, 2 × 2 cm² cuts of films were placed in a beaker containing 25 mL of 50% ethanol. Sampling was performed at room temperature (25 °C) with 1 h intervals. The solution (3 mL) was pulled out and replaced by fresh 50% ethanol. The sampling continued for the next 24 h [27]. The released curcumin from the film samples was assessed at 425 nm using a spectrophotometer (JASCO, Tokyo, Japan) [28].

2.5.6. Thermal Analysis

The thermal analysis of film samples and pure ingredients was conducted using a thermogravimetric analyzer (TGA-LABSYS EVO, SETARAM, Francelab, Budapest, Hungary). The experiment was performed under a nitrogen atmosphere with a 10 °C/min heating rate.

2.5.7. X-ray Diffraction (XRD)

The physical state of the film samples and pure ingredients was studied by XRD pattern obtained by an X-ray diffractometer (XRD-ASENWARE, AW-XDm300, Shenzhen, China). The equipment was operated with Cu-Kα ($\lambda = 1.54 \text{ \AA}$) under the voltage of 40 kV and 30 mA. The diffraction angular range for all samples was $2\theta = 5\text{--}60^\circ$ with a step size of $2\theta = 0.05^\circ$.

2.5.8. Fourier Transform Infrared (FTIR) Spectroscopy

FTIR spectra of the pure ingredients and the film samples were characterized by an FTIR spectrometer (FTIR-Jasco, Tokyo, Japan). All FTIR spectra were carried out at a resolution of 4 cm^{-1} and the spectral range of 4000 to 400 cm^{-1} .

2.6. Antioxidant Activity of Films

The antioxidant activity of film samples with and without curcumin was estimated based on hydrogen-donating ability, using the DPPH free-radical scavenging [29]. Briefly, 2 mL of each film solution was mixed with an equal volume of DPPH ethanolic solution (50 mg/L) and incubated in the dark for 30 min. DPPH solution and ethanol were mixed and used as blank. The absorbance was recorded at 517 nm using a spectrophotometer. DPPH radical scavenging capacity was determined using Equation (9):

$$\text{Free radical scavenging activity (\%)} = ((\text{Abs}_{\text{DPPH}} - \text{Abs}_{\text{sample}}) / \text{Abs}_{\text{DPPH}}) \times 100 \quad (9)$$

where $\text{Abs}_{\text{sample}}$ and Abs_{DPPH} are the absorbances of DPPH in film solution and blank, respectively.

2.7. Antibacterial Activity of Films

The antibacterial activity of the film samples was tested against 2 Gram-positive (*S. aureus* and *B. cereus*) and 2 Gram-negative (*S. Typhi* and *E. coli*) of the most common food-borne pathogenic bacteria [30]. First, all strains were incubated in TSB for 24 h at $37\text{ }^{\circ}\text{C}$. Then, the bacterial strains were diluted in MHB to obtain McFarland turbidity standard No. 0.5 (10^8 CFU/mL). These cultures were adjusted to the final concentration of bacterial cell suspension of 10^5 CFU/mL by diluting in MHB.

The antibacterial analysis was performed by agar disc diffusion and agar well diffusion. For the agar disc diffusion method, approximately $100\text{ }\mu\text{L}$ of prepared bacterial suspension was spread on solidified MHA surface by swab. The film samples were cut into a 6 mm diameter disc and placed on agar plates [31]. In addition, to evaluate antibacterial activity by agar well diffusion method, $100\text{ }\mu\text{L}$ of film solutions were poured into 6 mm diameter wells, which were punched on the plates containing MHA [32]. After 24 h incubation ($37\text{ }^{\circ}\text{C}$), the diameter of inhibition zone was determined by a digital micrometer (Mitutoyo, Kawasaki, Kanagawa, Japan). Triplicate measurements of antimicrobial activity were performed under the same conditions for each film sample.

2.8. Statistical Analysis

All investigations were performed in triplicate. The mean \pm standard deviation with the significant difference ($p < 0.05$) was determined by Duncan's multiple range test (SPSS statistical software, version 20).

3. Results and Discussion

3.1. Yield of Complex Coacervates

The PY of samples with different ratios of GE and SFTG were calculated (Table 1). The results showed a significant difference between the PY of samples ($p < 0.05$). It was varied in a range from 14.33 ± 0.81 to $60.06 \pm 0.14\%$. As far as GE content was enhanced, PY was improved. The yield in 1GE: 2SFTG ratio was significantly lower than two other samples. According to previous studies, the ratio of polymers in the complex coacervates affects complex yield. Furthermore, the lower balance of net charge and the weak interaction leads to formation of lower complex coacervates [33,34]. Based on the acquired results, the samples with higher PY (1GE: 1SFTG and 2GE: 1SFTG) were selected to produce films.

3.2. Physicochemical and Mechanical Properties of the Produced Active Films

3.2.1. Thickness and Mechanical Properties

The mechanical properties and thickness of all produced films are demonstrated in Table 2. There was no significant difference between the thickness of samples ($p < 0.05$). This might be related to the amount of curcumin, which was not enough to impact thickness. The authors of [35,36] also reported the same results. Mechanical properties are the key parameters in food packaging to have enough strength and flexibility to keep and carry the food [37]. As given in Table 2, there was no significant difference between film samples with curcumin (C1 and C2) and without it (F1 and F2) in TS and EAB ($p < 0.05$). After the addition of curcumin, the TS of F1 and F2 samples slightly decreased, possibly due to the intramolecular interaction of polymers with curcumin [35]. Other studies also indicated that TS declined after adding bioactive compounds [38–40]. By reducing TS, EAB (flexibility) increased due to the destruction of the intermolecular interaction between GE and SFTG when adding curcumin. The same finding was observed in tara gum/polyvinyl alcohol films incorporated with curcumin [41] and methylcellulose films containing α -tocopherol [38].

Table 2. Physical and mechanical properties of curcumin-loaded active film samples.

Film Samples	Thickness (mm)	WVP (g mm/kP Day m ²)	Moisture Content (%)	Water Solubility (%)	Tensile Strength (MPa)	Elongation at Break (%)
F1 (1GE: 1SFTG)	0.21 ± 0.06 ^a	0.6048 ± 0.12 ^a	63.67 ± 0.014 ^d	96.73 ± 1.11 ^d	1.74 ± 0.21 ^b	81.48 ± 2.91 ^a
C1 (1GE: 1SFTG/curcumin)	0.21 ± 0.02 ^a	0.4752 ± 0.15 ^a	54.14 ± 0.026 ^c	80.74 ± 1.21 ^c	0.62 ± 0.06 ^a	122.00 ± 11.81 ^b
F2 (2GE: 1SFTG)	0.25 ± 0.04 ^a	0.6912 ± 0.14 ^a	50.22 ± 0.025 ^b	78.80 ± 8.60 ^b	1.77 ± 0.48 ^b	98.87 ± 23.08 ^a
C2 (2GE: 1SFTG/curcumin)	0.25 ± 0.04 ^a	0.6048 ± 0.12 ^a	42.62 ± 0.057 ^a	35.93 ± 3.55 ^a	0.17 ± 0.07 ^a	109.58 ± 10.78 ^b

Different letters indicate significant differences ($p < 0.05$).

3.2.2. Water Vapor Permeability

The WVP is an important parameter representing the passage of water molecules through the films [42]. The WVP of film samples (Table 2) slightly decreased after adding curcumin, but the difference was not significant ($p > 0.05$). According to previous studies, adding hydrophobic compounds into composite films led to a lower WVP. In addition, a low amount of curcumin might have less impact on WVP values [35,43,44].

3.2.3. Moisture Content and Water Solubility

MC and WS of the film samples (Table 2) were influenced by different ratios of GE and SFTG with statistically significant differences ($p < 0.05$). The ranges of MC and WS were 42.62 ± 0.057 to 63.67 ± 0.014% and 35.93 ± 3.55 to 96.73 ± 1.11%, respectively. The samples containing more GE (F2 and C2) showed lower MC and WS than F1 and C1 samples. Additionally, a higher amount of gum in F1 and C1 samples caused an increase in MC and WS. The authors of [9] found that MC rose due to the increase in the amount of TG in films. In addition, the authors of [14] realized that adding more content of hydrophilic proteins to blended films reduced MC. Other researchers also proved that higher GE lessened WS of the film samples [45]. The authors of [46] studied chitosan/polyvinyl alcohol/fish gelatin films and demonstrated that the solubility of films reduced after the addition of fish gelatin. This was the result of reaction of polymers with hydrogen bonds, which led to lower free hydroxyl groups and lower bonding to water molecules. The control samples (F1 and F2) had significantly higher MC and WS compared to those with curcumin (C1 and C2) ($p < 0.05$). This finding was attributed to the hydrophobicity of curcumin,

which influenced the MC and WS of films. Similarly, other studies also elucidated that the addition of hydrophobic compounds tends to reduce MC [36,43] and WS [35,43] of blended films.

3.2.4. The Swelling Results of the Films

The swelling ratio (SR) of film samples is shown in Figure 1. The proportion of GE and SFTG showed a significant effect on SR. The maximum SR was observed for the film samples with an equal ratio of GE and SFTG (F1 and C1). The samples with the highest amount of GE (C2 and F2) presented the lowest SR. The control samples (F1 and F2) were able to uptake more water than samples with curcumin because of the hydrophilicity of polymers. Lee et al., (2004) evaluated different ratios of gellan and GE composite films and concluded that SR declined at higher content of GE [45], in agreement with the SR of GE/chitosan films [47]. After the addition of curcumin, which is a hydrophobic compound, the swelling capacity was enhanced. The presence of available hydrophilic groups and crystallinity of used materials impacted swelling behavior of the film samples. A similar trend was obtained for SR of curcumin/guar gum/polyhydroxyalkanoates composite films [48]. Similarly, incorporating curcumin into different carbohydrate films exhibited a bigger SR [35]. Other researchers also reported that the water absorbance of TG and GE films mounted as the content of gum was elevated. This is the result of a greater capacity to bond with the water molecules [9].

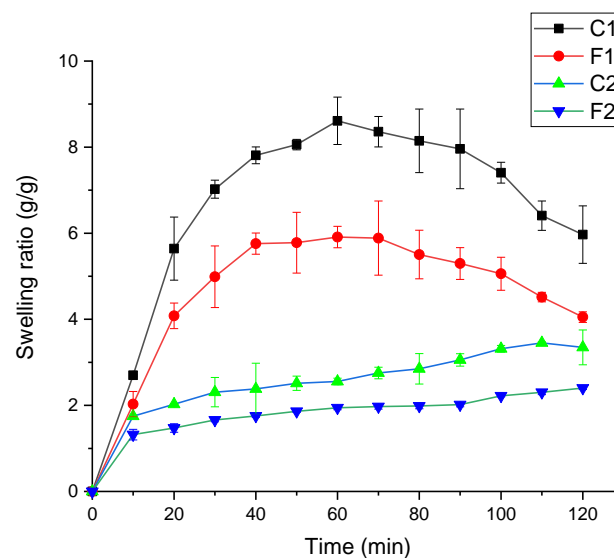


Figure 1. Swelling ratio of curcumin-loaded active film samples. F1 (1GE: 1SFTG); F2 (2GE: 1SFTG); C1 (1GE: 1 SFTG/curcumin); C2 (2GE: 1SFTG/curcumin).

3.2.5. Thermal Properties

The thermal stabilities of pure materials and different film samples are demonstrated in Figure 2. The first weight loss that occurred at <140 °C was related to moisture evaporation. For pure curcumin, the thermal degradation started at about 270 °C and reached 470 °C. The main thermal degradation of GE took place in the range of 260 to 450 °C. The original weight loss of SFTG started at about 220 °C, and 60% weight loss happened up to 450 °C. All film samples showed similar weight loss trends. The main weight loss of films (70%) started at about 200–300 °C, which was related to the depolymerization of polymers, and the final step of thermal decomposition (10%) was owing to the decomposition of film samples [49]. Incorporation of curcumin into films did not make a considerable difference in thermal stability compared to the pure film samples. Overall, the films showed lower thermal stability than pure materials. In agreement with this outcome, other researchers did not find any remarkable difference in the thermal stability of films with or without curcumin [35,50,51].

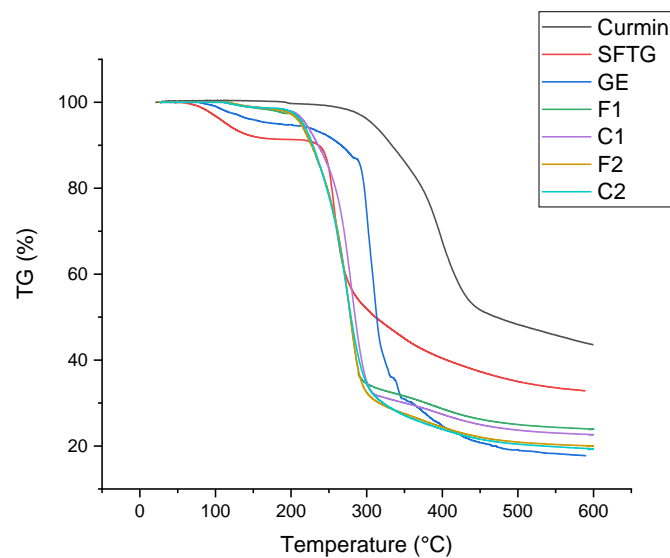


Figure 2. TGA of curcumin, SFTG, GE, and film samples. **F1** (1GE: 1SFTG); **F2** (2GE: 1SFTG); **C1** (1GE: 1 SFTG/curcumin); **C2** (2GE: 1SFTG/curcumin).

3.2.6. XRD Results

The XRD patterns of pure materials and various film samples are shown in Figure 3 as an indicator for evaluating their crystallinity. The XRD pattern of SFTG revealed maximum peak intensity at 13.7° and a broader peak at 30.35° . This result showed the amorphous nature of SFTG with an almost crystalline (or a crystalline-like) part. A broad curve at around $2\theta \approx 20^\circ$ was observed in the XRD pattern of GE. According to previous studies, this is attributed to the α -helix and triple-helical structure of GE, which causes a semicrystalline structure [52]. Regarding curcumin, some highlighted peaks appeared in the region of $2\theta \approx 12.25^\circ$ – 29° in its XRD pattern. Thus, the structure of curcumin was considered crystalline [53]. All film samples depicted amorphous structure, and the semicrystalline pattern of their individual components was eliminated. In addition, it was observed that the crystalline peaks of curcumin did not emerge in C1 and C2 samples. This indicated successful interaction between biopolymers and curcumin.

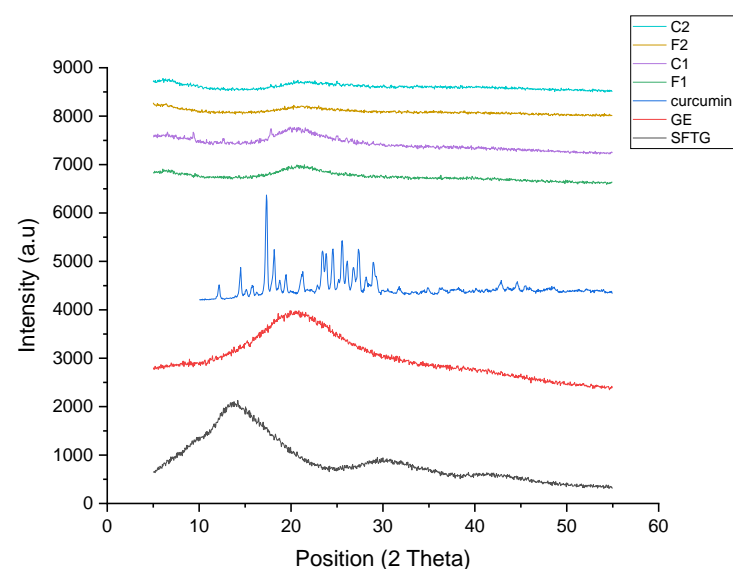


Figure 3. XRD patterns of curcumin, SFTG, GE, and film samples. **F1** (1GE: 1SFTG); **F2** (2GE: 1SFTG); **C1** (1GE: 1 SFTG/curcumin); **C2** (2GE: 1SFTG/curcumin).

3.2.7. Chemical and Functional Groups of the Films

The functional groups of GE, SFTG, and curcumin and their interactions in the film samples were characterized by FTIR (Figure 4). In the case of GE, the peaks at around 1666, 1513, and 1232 cm^{-1} were associated with amide I (C=O and C-N), amide II (N-H and C-N), and amide III (N-H and C-N), respectively. Additionally, the absorption peaks at almost 3410 and 3071 cm^{-1} were ascribed to the amide A, and amide B of GE, respectively [20,54,55]. FTIR spectroscopy of SFTG revealed the carbohydrate characteristic peaks in the area of 908–1248 cm^{-1} . The bands at about 1612 and 1444 cm^{-1} belonged to the carboxylic group (-COO). Moreover, SFTG displayed a peak at 1748 cm^{-1} which is due to the C=O group. The peaks that appeared at around 3438 and 2923 cm^{-1} corresponded to the hydroxyl (-OH) and methylene group absorption bands, respectively [56]. The curcumin spectrum depicted a band at approximately 1627 cm^{-1} that contributed to the overlapping alkenes and carbonyl groups. The peak at 1600 cm^{-1} appeared due to benzene ring stretching vibration. Furthermore, the bending vibration of the C-H group and C-O and C-O-C stretching vibration were revealed at 1431, 1280, and 1026 cm^{-1} , respectively. The emerging peaks at 3419–3508 cm^{-1} were related to O-H groups [57,58].

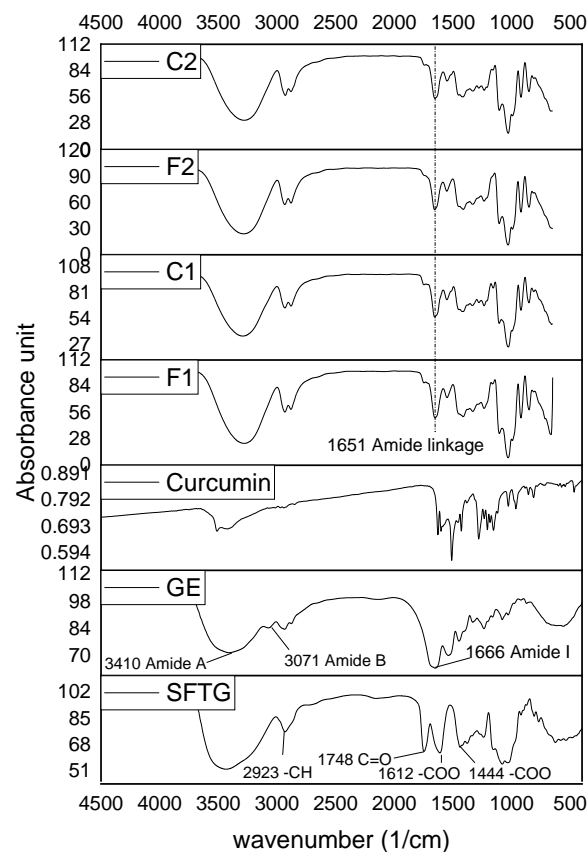


Figure 4. FTIR spectra of curcumin, SFTG, GE, and film samples. **F1** (1GE: 1SFTG); **F2** (2GE: 1SFTG); **C1** (1GE: 1 SFTG/curcumin); **C2** (2GE: 1SFTG/curcumin).

All film samples showed approximately similar FTIR spectra. At first glance, it is obvious that some peaks disappeared and shifted, which might be a consequence of some chemical reactions. Accordingly, the reaction between the carboxylic group of SFTG and amide I of GE formed an amide linkage which showed a slight shift from 1666 cm^{-1} in GE to 1652 cm^{-1} in all films, respectively [59,60]. Moreover, the amide A band (3410 cm^{-1}) in GE shifted in all film samples. This might be a result of bonding the hydroxyl group of SFTG and glycerol with amine groups of GE. A similar observation was found by [59,61]. Amide B did not appear in any of the film samples, which may be due to hydroxyl group interactions [59].

3.3. Release Results of Curcumin from Active Films

The release of curcumin from the films into 50% ethanol (fatty food simulants) is elucidated in Figure 5. As is clear, the cumulative amount of released curcumin was very low and <2% of its release was after 24 h. Most of the curcumin release happened in the first 15 min. The release trend of C1 samples was very similar to C2. Various factors impact the release of bioactive ingredients from the base matrix, such as the type of polymers, the interaction of film compounds, the swelling rate, and the solubility of film samples [62]. In addition, the increasing rate of release is expected to continue after 24 h.

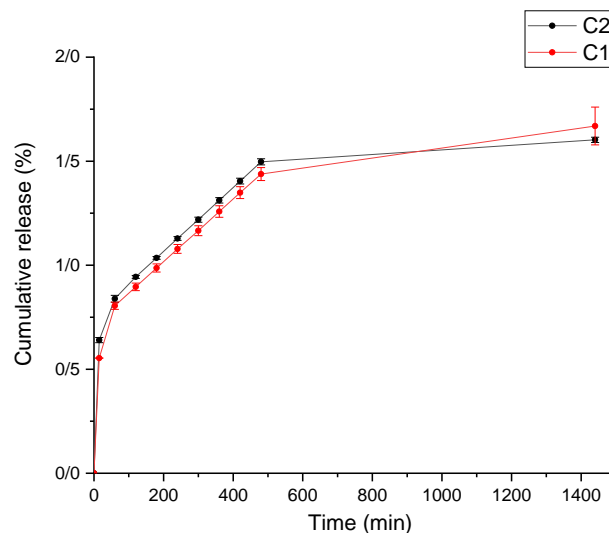


Figure 5. Release of curcumin from composite films in 50% ethanol fatty food simulant. **C1** (1GE: 1 SFTG/curcumin); **C2** (2GE: 1SFTG/curcumin).

3.4. Antioxidant Activity of Curcumin-Loaded Films

The pure film samples (F1 and F2) revealed approximately 15% antioxidant activity (Figure 6). After loading of curcumin, the antioxidant capacity of films improved strikingly. The antioxidant feature of C1 and C2 samples was 80.9% and 74.6%, respectively. The antioxidant capacity of curcumin corresponds to its donation of H atom from phenolic groups [63]. The proportion of biopolymers in film complexes did not significantly affect this property. Previously, it was reported that adding curcumin into carbohydrate-based films caused a noticeable rise in their antioxidant activity [35]. Moreover, a remarkable increase in antioxidant activity was found in GE/curcumin edible packaging [43,51]. Other researchers also prepared films with different biopolymers incorporating curcumin, which resulted in high antioxidant activity [41,64,65].

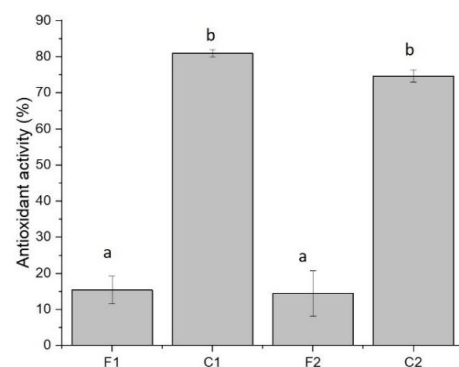


Figure 6. Antioxidant activity of film samples containing curcumin. **F1** (1GE: 1SFTG); **F2** (2GE: 1SFTG); **C1** (1GE: 1 SFTG/curcumin); **C2** (2GE: 1SFTG/curcumin). Different letters show significantly different ($p < 0.05$).

3.5. Antibacterial Activity of Curcumin-Loaded Films

The film samples showed no antibacterial activity against tested bacteria. This result could be related to the low concentration of curcumin in the studied films. Moreover, the interaction of curcumin with biopolymers may hinder the release of curcumin, which results in a lack of antibacterial activity. Musso et al., (2016), who surveyed the smart GE edible films containing 0.02 *w/v* curcumin, detected similar findings [43]. In another study, researchers indicated that sunflower protein films incorporated with phenolic compounds of sunflower seeds did not affect bacterial strains because phenolic compounds were bonded with protein [66]. The antibacterial effect of curcumin that incorporated poly (butylene adipate-co-terephthalate) was also insignificant, although it revealed a slight enhancement by raising the amount of curcumin [65]. In other studies in which curcumin content was higher than this research, a considerable antimicrobial consequence was observed against Gram-positive and Gram-negative bacteria [40,50].

4. Conclusions

Active packaging films were made by complex coacervation of SFTG and GE loaded with curcumin. Although the curcumin-loaded films did not show any antibacterial activity, they presented a great antioxidant activity (around 80%). This result could be attributed to the low concentration of curcumin in the studied films, and higher concentrations of curcumin in active packaging are suggested to improve the antimicrobial activity. The cumulative release of curcumin from films in 50% ethanol fatty simulants increased steadily during 24 h. The present work outcomes revealed the potential use of the obtained film samples in antioxidant packaging to prolong the shelf-life of fatty food due to the high efficiency of the released curcumin.

Author Contributions: Conceptualization, A.R. and S.M.J.; methodology, A.R., F.A., H.A.; software, A.R.; validation, A.R.; formal analysis, A.R.; investigation, A.R., F.A., H.A.; resources, A.R.; data curation, A.R., F.A.; writing—original draft preparation, A.R., F.A.; writing—review and editing, A.R., S.M.J.; visualization, A.R., S.M.J. and C.D.; supervision, A.R. and S.M.J.; project administration, A.R.; funding acquisition, A.R. All authors have read and agreed to the published version of the manuscript.

Funding: This research was funded by Isfahan University of Medical Sciences (grant number 2400192).

Data Availability Statement: Data is contained within the article.

Conflicts of Interest: The authors declare no conflict of interest.

References

1. Bhargava, N.; Sharanagat, V.S.; Mor, R.S.; Kumar, K. Active and intelligent biodegradable packaging films using food and food waste-derived bioactive compounds: A review. *Trends Food Sci. Technol.* **2020**, *105*, 385–401. [[CrossRef](#)]
2. Sani, M.A.; Azizi-Lalabadi, M.; Tavassoli, M.; Mohammadi, K.; McClements, D.J. Recent advances in the development of smart and active biodegradable packaging materials. *Nanomaterials* **2021**, *11*, 1331. [[CrossRef](#)] [[PubMed](#)]
3. Ivonkovic, A.; Zeljko, K.; Talic, S.; Lasic, M. Biodegradable packaging in the food industry. *J. Food Saf. Food Qual.* **2017**, *68*, 26–38.
4. Nesterenko, A.; Alric, I.; Silvestre, F.; Durrieu, V. Vegetable proteins in microencapsulation: A review of recent interventions and their effectiveness. *Ind. Crops Prod.* **2013**, *42*, 469–479. [[CrossRef](#)]
5. Ahmed, S.; Ikram, S. Chitosan and gelatin based biodegradable packaging films with UV-light protection. *J. Photochem. Photobiol. B Biol.* **2016**, *163*, 115–124. [[CrossRef](#)] [[PubMed](#)]
6. Kumar, S.; Shukla, A.; Baul, P.P.; Mitra, A.; Halder, D. Biodegradable hybrid nanocomposites of chitosan/gelatin and silver nanoparticles for active food packaging applications. *Food Packag. Shelf Life* **2018**, *16*, 178–184. [[CrossRef](#)]
7. Mohammadifar, M.A.; Musavi, S.M.; Kiumarsi, A.; Williams, P.A. Solution properties of targacanthin (water-soluble part of gum tragacanth exudate from *Astragalus gossypinus*). *Int. J. Biol. Macromol.* **2006**, *38*, 31–39. [[PubMed](#)]
8. Karimi, N.; Mohammadifar, M.A. Role of water soluble and water swellable fractions of gum tragacanth on stability and characteristic of model oil in water emulsion. *Food Hydrocoll.* **2014**, *37*, 124–133. [[CrossRef](#)]
9. Khodaei, D.; Oltrogge, K.; Hamidi-Esfahani, Z. Preparation and characterization of blended edible films manufactured using gelatin, tragacanth gum and, Persian gum. *LWT* **2020**, *117*, 108617. [[CrossRef](#)]

10. Gentile, L. Protein–polysaccharide interactions and aggregates in food formulations. *Curr. Opin. Colloid Interface Sci.* **2020**, *48*, 18–27.
11. Wei, Z.; Huang, Q. Assembly of protein–polysaccharide complexes for delivery of bioactive ingredients: A perspective paper. *J. Agric. Food Chem.* **2019**, *67*, 1344–1352. [[CrossRef](#)]
12. Schmitt, C.; Turgeon, S.L. Protein/polysaccharide complexes and coacervates in food systems. *Adv. Colloid Interface Sci.* **2011**, *167*, 63–70. [[CrossRef](#)]
13. Weinbreck, F.; De Vries, R.; Schrooyen, P.; De Kruif, C. Complex coacervation of whey proteins and gum arabic. *Biomacromolecules* **2003**, *4*, 293–303. [[CrossRef](#)]
14. Eghbal, N.; Yarmand, M.S.; Mousavi, M.; Degraeve, P.; Oulahal, N.; Gharsallaoui, A. Complex coacervation for the development of composite edible films based on LM pectin and sodium caseinate. *Carbohydr. Polym.* **2016**, *151*, 947–956. [[CrossRef](#)]
15. Tavares, L.; Souza, H.K.; Gonçalves, M.P.; Rocha, C.M. Physicochemical and microstructural properties of composite edible film obtained by complex coacervation between chitosan and whey protein isolate. *Food Hydrocoll.* **2021**, *113*, 106471. [[CrossRef](#)]
16. Stohs, S.J.; Chen, O.; Ray, S.D.; Ji, J.; Bucci, L.R.; Preuss, H.G. Highly bioavailable forms of curcumin and promising avenues for curcumin-based research and application: A review. *Molecules* **2020**, *25*, 1397. [[CrossRef](#)]
17. Sharifi, S.; Fathi, N.; Memar, M.Y.; Hosseiniyan Khatibi, S.M.; Khalilov, R.; Negahdari, R.; Zununi Vahed, S.; Maleki Dizaj, S. Anti-microbial activity of curcumin nanoformulations: New trends and future perspectives. *Phytother. Res.* **2020**, *34*, 1926–1946. [[CrossRef](#)]
18. Soleimani, V.; Sahebkar, A.; Hosseinzadeh, H. Turmeric (*Curcuma longa*) and its major constituent (curcumin) as nontoxic and safe substances. *Phytother. Res.* **2018**, *32*, 985–995. [[CrossRef](#)]
19. Rezaei, A.; Nasirpour, A.; Tavanai, H. Fractionation and some physicochemical properties of almond gum (*Amygdalus communis* L.) exudates. *Food Hydrocoll.* **2016**, *60*, 461–469. [[CrossRef](#)]
20. Devi, N.; Maji, T.K. Genipin crosslinked microcapsules of gelatin A and κ -carrageenan polyelectrolyte complex for encapsulation of Neem (*Azadirachta Indica* A. Juss.) seed oil. *Polym. Bull.* **2010**, *65*, 347–362. [[CrossRef](#)]
21. ASTM D882-02; Standard Test Method for Tensile Properties of Thin Plastic Sheeting. ASTM: West Conshohocken, PA, USA, 1995.
22. ASTM. Standard test method for water vapor transmission of materials. In *Annual Books of ASTM Standards. Designation E 96-01*, Philadelphia: ASTM, American Society for Testing Materials; ASTM: West Conshohocken, PA, USA, 2001.
23. Haghighi, H.; Biard, S.; Bigi, F.; De Leo, R.; Bedin, E.; Pfeifer, F.; Siesler, H.W.; Licciardello, F.; Pulvirenti, A. Comprehensive characterization of active chitosan–gelatin blend films enriched with different essential oils. *Food Hydrocoll.* **2019**, *95*, 33–42. [[CrossRef](#)]
24. Łupina, K.; Kowalczyk, D.; Drozłowska, E. Polysaccharide/gelatin blend films as carriers of ascorbyl palmitate—A comparative study. *Food Chem.* **2020**, *333*, 127465. [[CrossRef](#)] [[PubMed](#)]
25. Kochkina, N.E.; Lukin, N.D. Structure and properties of biodegradable maize starch/chitosan composite films as affected by PVA additions. *Int. J. Biol. Macromol.* **2020**, *157*, 377–384. [[CrossRef](#)] [[PubMed](#)]
26. European Food Safety Authority (EFSA). Opinion of the Scientific Panel on food additives, flavourings, processing aids and materials in contact with food (AFC) related to a 16th list of substances for food contact materials. *EFSA J.* **2007**, *5*, 555. [[CrossRef](#)]
27. Amani, F.; Sami, M.; Rezaei, A. Characterization and antibacterial activity of encapsulated rosemary essential oil within amylose nanostructures as a natural antimicrobial in food applications. *Starch-Stärke* **2021**, *73*, 2100021. [[CrossRef](#)]
28. Rezaei, A.; Nasirpour, A. Evaluation of release kinetics and mechanisms of curcumin and curcumin- β -cyclodextrin inclusion complex incorporated in electrospun almond gum/PVA nanofibers in simulated saliva and simulated gastrointestinal conditions. *BioNanoScience* **2019**, *9*, 438–445. [[CrossRef](#)]
29. Brand-Williams, W.; Cuvelier, M.-E.; Berset, C. Use of a free radical method to evaluate antioxidant activity. *LWT—Food Sci. Technol.* **1995**, *28*, 25–30. [[CrossRef](#)]
30. Bintsis, T. Foodborne pathogens. *AIMS Microbiol.* **2017**, *3*, 529–563. [[CrossRef](#)]
31. Hanani, Z.N.; Yee, F.C.; Nor-Khaizura, M. Effect of pomegranate (*Punica granatum* L.) peel powder on the antioxidant and antimicrobial properties of fish gelatin films as active packaging. *Food Hydrocoll.* **2019**, *89*, 253–259. [[CrossRef](#)]
32. Rukmanikrishnan, B.; Ramalingam, S.; Lee, J. Quaternary ammonium silane-reinforced agar/polyacrylamide composites for packaging applications. *Int. J. Biol. Macromol.* **2021**, *182*, 1301–1309. [[CrossRef](#)]
33. Eratte, D.; Wang, B.; Dowling, K.; Barrow, C.J.; Adhikari, B.P. Complex coacervation with whey protein isolate and gum arabic for the microencapsulation of omega-3 rich tuna oil. *Food Funct.* **2014**, *5*, 2743–2750. [[CrossRef](#)]
34. Shinde, U.A.; Nagarsenker, M.S. Characterization of gelatin–sodium alginate complex coacervation system. *Indian J. Pharm. Sci.* **2009**, *71*, 313.
35. Roy, S.; Rhim, J.-W. Preparation of carbohydrate-based functional composite films incorporated with curcumin. *Food Hydrocoll.* **2020**, *98*, 105302. [[CrossRef](#)]
36. Wu, J.; Sun, X.; Guo, X.; Ji, M.; Wang, J.; Cheng, C.; Chen, L.; Wen, C.; Zhang, Q. Physicochemical, antioxidant, in vitro release, and heat sealing properties of fish gelatin films incorporated with β -cyclodextrin/curcumin complexes for apple juice preservation. *Food Bioprocess Technol.* **2018**, *11*, 447–461.
37. Kanatt, S.R.; Rao, M.; Chawla, S.; Sharma, A. Active chitosan–polyvinyl alcohol films with natural extracts. *Food Hydrocoll.* **2012**, *29*, 290–297. [[CrossRef](#)]

38. Noronha, C.M.; de Carvalho, S.M.; Lino, R.C.; Barreto, P.L.M. Characterization of antioxidant methylcellulose film incorporated with α -tocopherol nanocapsules. *Food Chem.* **2014**, *159*, 529–535. [[CrossRef](#)]
39. Martins, J.T.; Cerqueira, M.A.; Vicente, A.A. Influence of α -tocopherol on physicochemical properties of chitosan-based films. *Food Hydrocoll.* **2012**, *27*, 220–227.
40. Luo, N.; Varaprasad, K.; Reddy, G.V.S.; Rajulu, A.V.; Zhang, J. Preparation and characterization of cellulose/curcumin composite films. *RSC Adv.* **2012**, *2*, 8483–8488. [[CrossRef](#)]
41. Ma, Q.; Ren, Y.; Wang, L. Investigation of antioxidant activity and release kinetics of curcumin from tara gum/polyvinyl alcohol active film. *Food Hydrocoll.* **2017**, *70*, 286–292.
42. Atef, M.; Rezaei, M.; Behrooz, R. Characterization of physical, mechanical, and antibacterial properties of agar-cellulose bionanocomposite films incorporated with savory essential oil. *Food Hydrocoll.* **2015**, *45*, 150–157.
43. Musso, Y.S.; Salgado, P.R.; Mauri, A.N. Smart edible films based on gelatin and curcumin. *Food Hydrocoll.* **2017**, *66*, 8–15. [[CrossRef](#)]
44. Da Silva, M.N.; de Matos Fonseca, J.; Feldhaus, H.K.; Soares, L.S.; Valencia, G.A.; de Campos, C.E.M.; Di Luccio, M.; Monteiro, A.R. Physical and morphological properties of hydroxypropyl methylcellulose films with curcumin polymorphs. *Food Hydrocoll.* **2019**, *97*, 105217. [[CrossRef](#)]
45. Lee, K.Y.; Shim, J.; Lee, H.G. Mechanical properties of gellan and gelatin composite films. *Carbohydr. Polym.* **2004**, *56*, 251–254. [[CrossRef](#)]
46. Ghaderi, J.; Hosseini, S.F.; Keyvani, N.; Gómez-Guillén, M.C. Polymer blending effects on the physicochemical and structural features of the chitosan/poly (vinyl alcohol)/fish gelatin ternary biodegradable films. *Food Hydrocoll.* **2019**, *95*, 122–132. [[CrossRef](#)]
47. Koc, F.E.; Altınçekic, T.G. Investigation of gelatin/chitosan as potential biodegradable polymer films on swelling behavior and methylene blue release kinetics. *Polym. Bull.* **2021**, *78*, 3383–3398. [[CrossRef](#)]
48. Pramanik, N.; Mitra, T.; Khamrai, M.; Bhattacharyya, A.; Mukhopadhyay, P.; Gnanamani, A.; Basu, R.K.; Kundu, P.P. Characterization and evaluation of curcumin loaded guar gum/polyhydroxyalkanoates blend films for wound healing applications. *RSC Adv.* **2015**, *5*, 63489–63501. [[CrossRef](#)]
49. Türe, H. Characterization of hydroxyapatite-containing alginate–gelatin composite films as a potential wound dressing. *Int. J. Biol. Macromol.* **2019**, *123*, 878–888. [[CrossRef](#)]
50. Roy, S.; Rhim, J.-W. Antioxidant and antimicrobial poly (vinyl alcohol)-based films incorporated with grapefruit seed extract and curcumin. *J. Environ. Chem. Eng.* **2021**, *9*, 104694. [[CrossRef](#)]
51. Roy, S.; Rhim, J.-W. Preparation of antimicrobial and antioxidant gelatin/curcumin composite films for active food packaging application. *Colloids Surf. B Biointerfaces* **2020**, *188*, 110761. [[CrossRef](#)]
52. Ki, C.S.; Baek, D.H.; Gang, K.D.; Lee, K.H.; Um, I.C.; Park, Y.H. Characterization of gelatin nanofiber prepared from gelatin–formic acid solution. *Polymer* **2005**, *46*, 5094–5102.
53. Rezaei, A.; Nasirpour, A. Encapsulation of curcumin using electrospun almond gum nanofibers: Fabrication and characterization. *Int. J. Food Prop.* **2018**, *21*, 1608–1618. [[CrossRef](#)]
54. Riaz, T.; Zeeshan, R.; Zarif, F.; Ilyas, K.; Muhammad, N.; Safi, S.Z.; Rahim, A.; Rizvi, S.A.; Rehman, I.U. FTIR analysis of natural and synthetic collagen. *Appl. Spectrosc. Rev.* **2018**, *53*, 703–746. [[CrossRef](#)]
55. Derkach, S.R.; Voron'ko, N.G.; Sokolan, N.I.; Kolotova, D.S.; Kuchina, Y.A. Interactions between gelatin and sodium alginate: UV and FTIR studies. *J. Dispers. Sci. Technol.* **2019**, *41*, 690–698. [[CrossRef](#)]
56. Nowrouzi, I.; Manshad, A.K.; Mohammadi, A.H. Effects of Tragacanth Gum as a natural polymeric surfactant and soluble ions on chemical smart water injection into oil reservoirs. *J. Mol. Struct.* **2020**, *1200*, 127078. [[CrossRef](#)]
57. Chen, X.; Zou, L.-Q.; Niu, J.; Liu, W.; Peng, S.-F.; Liu, C.-M. The stability, sustained release and cellular antioxidant activity of curcumin nanoliposomes. *Molecules* **2015**, *20*, 14293–14311. [[CrossRef](#)]
58. Ismail, E.; Sabry, D.; Mahdy, H.; Khalil, M. Synthesis and Characterization of some ternary metal complexes of curcumin with 1, 10-phenanthroline and their anticancer applications. *J. Sci. Res.* **2014**, *6*, 509–519. [[CrossRef](#)]
59. Hazirah, M.N.; Isa, M.; Sarbon, N. Effect of xanthan gum on the physical and mechanical properties of gelatin-carboxymethyl cellulose film blends. *Food Packag. Shelf Life* **2016**, *9*, 55–63. [[CrossRef](#)]
60. Ahmed, J.; Mulla, M.; Joseph, A.; Ejaz, M.; Maniruzzaman, M. Zinc oxide/clove essential oil incorporated type B gelatin nanocomposite formulations: A proof-of-concept study for 3D printing applications. *Food Hydrocoll.* **2020**, *98*, 105256. [[CrossRef](#)]
61. Zhong, Q.-P.; Xia, W.-S. Physicochemical properties of edible and preservative films from chitosan/cassava starch/gelatin blend plasticized with glycerol. *Food Technol. Biotechnol.* **2008**, *46*, 262–269.
62. Wang, L.-F.; Rhim, J.-W. Grapefruit seed extract incorporated antimicrobial LDPE and PLA films: Effect of type of polymer matrix. *LWT* **2016**, *74*, 338–345. [[CrossRef](#)]
63. Ak, T.; Gülçin, İ. Antioxidant and radical scavenging properties of curcumin. *Chem. Biol. Interact.* **2008**, *174*, 27–37. [[CrossRef](#)]
64. Zia, J.; Paul, U.C.; Heredia-Guerrero, J.A.; Athanassiou, A.; Fragouli, D. Low-density polyethylene/curcumin melt extruded composites with enhanced water vapor barrier and antioxidant properties for active food packaging. *Polymer* **2019**, *175*, 137–145. [[CrossRef](#)]

-
65. Roy, S.; Rhim, J.-W. Curcumin incorporated poly (butylene adipate-co-terephthalate) film with improved water vapor barrier and antioxidant properties. *Materials* **2020**, *13*, 4369.
 66. Salgado, P.R.; López-Caballero, M.E.; Gómez-Guillén, M.C.; Mauri, A.N.; Montero, M.P. Exploration of the antioxidant and antimicrobial capacity of two sunflower protein concentrate films with naturally present phenolic compounds. *Food Hydrocoll.* **2012**, *29*, 374–381. [[CrossRef](#)]